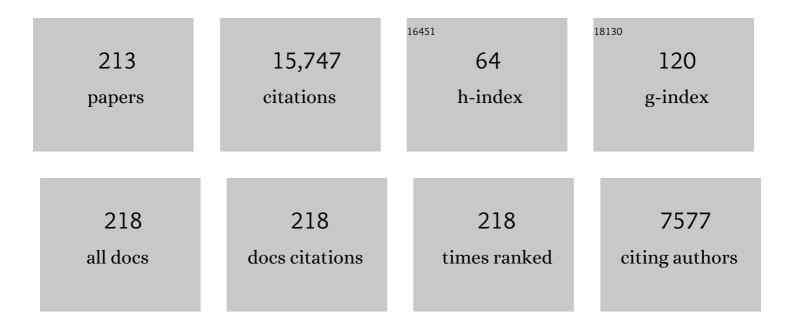
Trevor R Ireland

List of Publications by Year in descending order

Source: https://exaly.com/author-pdf/1253014/publications.pdf Version: 2024-02-01



#	Article	IF	CITATIONS
1	Samples returned from the asteroid Ryugu are similar to Ivuna-type carbonaceous meteorites. Science, 2023, 379, .	12.6	97
2	The Paleoarchean Northern Mundo Novo Greenstone Belt, São Francisco Craton: Geochemistry, U–Pb–Hf–O in zircon and pyrite Î′34S-Δ33S-Δ36S signatures. Geoscience Frontiers, 2022, 13, 101252.	8.4	3
3	Foulwind Suite magmatism in the Buller Terrane, New Zealand: geochemistry of the Carboniferous Foulwind and Windy Point Granites. New Zealand Journal of Geology, and Geophysics, 2022, 65, 470-490.	1.8	2
4	Solid-phase transfer into the forearc mantle wedge: Rutile and zircon xenocrysts fingerprint subducting sources. Earth and Planetary Science Letters, 2022, 577, 117251.	4.4	10
5	A Model Earth-sized Planet in the Habitable Zone of α Centauri A/B. Astrophysical Journal, 2022, 927, 134.	4.5	4
6	Direct dating of podiform Chromitite: U-Pb (Zircon, Rutile) and 40Ar/39Ar (Pargasite) evidence from Tiébaghi Cr deposit (New Caledonia). Ore Geology Reviews, 2022, 145, 104873.	2.7	2
7	Preliminary analysis of the Hayabusa2 samples returned from C-type asteroid Ryugu. Nature Astronomy, 2022, 6, 214-220.	10.1	136
8	Strontium isotope analysis of apatite via SIMS. Chemical Geology, 2021, 559, 119979.	3.3	14
9	Sources of auriferous fluids associated with a Neoarchean BIF-hosted orogenic gold deposit revealed by the multiple sulfur isotopic compositions of zoned pyrites. Contributions To Mineralogy and Petrology, 2021, 176, 1.	3.1	2
10	A petrochronology window into near-surface fluid/rock interaction within Archaean ultramafic-mafic crust: Insights from the 3.25ÂGa Stolzburg Complex, Barberton Greenstone Belt. Chemical Geology, 2021, 569, 120130.	3.3	6
11	Geochronological constrains on the timing of magmatism, deformation and mineralization at the Karouni orogenic gold deposit: Guyana, South America. Precambrian Research, 2020, 337, 105329.	2.7	8
12	Highâ€Precision, Highâ€Accuracy Oxygen Isotope Measurements of Zircon Reference Materials with the SHRIMPâ€SI. Geostandards and Geoanalytical Research, 2020, 44, 85-102.	3.1	21
13	Cretaceous molybdenite in metasomatic epidosite associated with the Pounamu ophiolite, New Zealand. New Zealand Journal of Geology, and Geophysics, 2020, 63, 227-236.	1.8	1
14	The sign of Δ33S is independent of pyrite morphology. Chemical Geology, 2020, 532, 119369.	3.3	1
15	Structure and evolution of the Wairakei–Tauhara geothermal system (Taupo Volcanic Zone, New) Tj ETQq1 1 Research, 2020, 390, 106705.	0.784314 2.1	rgBT /Overlo 16
16	SW Pacific arc and backarc lavas and the role of slab-bend serpentinites in the global halogen cycle. Earth and Planetary Science Letters, 2020, 530, 115921.	4.4	22
17	Protocols for in situ measurement of oxygen isotopes in goethite by ion microprobe. Chemical Geology, 2020, 533, 119436.	3.3	2
18	A zircon U-Pb geochronology for the Rotokawa geothermal system, New Zealand, with implications for TaupŕVolcanic Zone evolution. Journal of Volcanology and Geothermal Research, 2020, 389, 106729.	2.1	19

#	Article	IF	CITATIONS
19	Magnesium in subaqueous speleothems as a potential palaeotemperature proxy. Nature Communications, 2020, 11, 5027.	12.8	16
20	In-situ quadruple sulfur isotopic compositions of pyrites in the ca. 3.2–2.72ÂGa metasedimentary rocks from the Pilbara Craton, Western Australia. Chemical Geology, 2020, 557, 119837.	3.3	2
21	Exploring the efficiency of stepwise dissolution in removal of stubborn non-radiogenic Pb in chondrule U-Pb dating. Geochimica Et Cosmochimica Acta, 2020, 277, 1-20.	3.9	10
22	Triple oxygen isotope variations in magnetite from iron-oxide deposits, central Iran, record magmatic fluid interaction with evaporite and carbonate host rocks. Geology, 2020, 48, 211-215.	4.4	34
23	New U Pb, Hf and O isotope constraints on the provenance of sediments from the Adelaide Rift Complex – Documenting the key Neoproterozoic to early Cambrian succession. Gondwana Research, 2020, 83, 248-278.	6.0	20
24	Geochemical characteristics of pyrite in the Dabaozhuang deposit in the Middle-Lower Yangtze River Metallogenic Belt, Eastern China. Ore Geology Reviews, 2020, 124, 103662.	2.7	8
25	Oxygen Isotopes and Sampling of the Solar System. Space Science Reviews, 2020, 216, 1.	8.1	22
26	Textural and geochemical investigation of pyrite in Jacobina Basin, São Francisco Craton, Brazil: Implications for paleoenvironmental conditions and formation of pre-GOE metaconglomerate-hosted Au-(U) deposits. Geochimica Et Cosmochimica Acta, 2020, 273, 331-353.	3.9	9
27	Quadruple sulfur isotopic fractionation during pyrite desulfidation to pyrrhotite. Geochimica Et Cosmochimica Acta, 2020, 273, 354-366.	3.9	9
28	Hydrothermal fluid characteristics and implications of the Makou IOA deposit in Luzong Basin, eastern China. Ore Geology Reviews, 2020, 127, 103867.	2.7	2
29	Thermal history of Early Jurassic eclogite facies metamorphism in the Nagaland Ophiolite Complex, NE India: New insights into pre-Cretaceous subduction channel tectonics within the Neo-Tethys. Lithos, 2019, 346-347, 105166.	1.4	16
30	Global atmospheric oxygen variations recorded by Th/U systematics of igneous rocks. Proceedings of the United States of America, 2019, 116, 18854-18859.	7.1	40
31	Pyrite trace-element and sulfur isotope geochemistry of paleo-mesoproterozoic McArthur Basin: Proxy for oxidative weathering. American Mineralogist, 2019, 104, 1256-1272.	1.9	28
32	Mesoarchaean clockwise metamorphic P-T path from the Western Dharwar Craton. Lithos, 2019, 342-343, 370-390.	1.4	12
33	The formation mechanisms of sedimentary pyrite nodules determined by trace element and sulfur isotope microanalysis. Geochimica Et Cosmochimica Acta, 2019, 259, 53-68.	3.9	53
34	Best practices for the use of meteorite names in publications. Meteoritics and Planetary Science, 2019, 54, 1397-1400.	1.6	2
35	Tectonic Evolution of the Western Margin of the Burma Microplate Based on New Fossil and Radiometric Age Constraints. Tectonics, 2019, 38, 1718-1741.	2.8	59
36	Comparative geochemical study of scheelite from the Shizhuyuan and Xianglushan tungsten skarn deposits, South China: Implications for scheelite mineralization. Ore Geology Reviews, 2019, 109, 448-464.	2.7	36

#	Article	IF	CITATIONS
37	The operational environment and rotational acceleration of asteroid (101955) Bennu from OSIRIS-REx observations. Nature Communications, 2019, 10, 1291.	12.8	99
38	The dynamic geophysical environment of (101955) Bennu based on OSIRIS-REx measurements. Nature Astronomy, 2019, 3, 352-361.	10.1	132
39	Evidence for widespread hydrated minerals on asteroid (101955) Bennu. Nature Astronomy, 2019, 3, 332-340.	10.1	251
40	Properties of rubble-pile asteroid (101955) Bennu from OSIRIS-REx imaging and thermal analysis. Nature Astronomy, 2019, 3, 341-351.	10.1	188
41	Craters, boulders and regolith of (101955) Bennu indicative of an old and dynamic surface. Nature Geoscience, 2019, 12, 242-246.	12.9	161
42	Shape of (101955) Bennu indicative of a rubble pile with internal stiffness. Nature Geoscience, 2019, 12, 247-252.	12.9	179
43	The unexpected surface of asteroid (101955) Bennu. Nature, 2019, 568, 55-60.	27.8	364
44	The volatility trend of protosolar and terrestrial elemental abundances. Icarus, 2019, 328, 287-305.	2.5	21
45	U-Th/He systematics of fluid-rich †fibrous' diamonds – Evidence for pre- and syn-kimberlite eruption ages. Chemical Geology, 2019, 515, 22-36.	3.3	11
46	Mineralogical constraints on the thermal history of martian regolith breccia Northwest Africa 8114. Geochimica Et Cosmochimica Acta, 2019, 246, 267-298.	3.9	12
47	Reconnaissance Basement Geology and Tectonics of South Zealandia. Tectonics, 2019, 38, 516-551.	2.8	46
48	Enhanced constraints on the interior composition and structure of terrestrial exoplanets. Monthly Notices of the Royal Astronomical Society, 2019, 482, 2222-2233.	4.4	25
49	Major Miocene geological events in southern Tibet and eastern Asia induced by the subduction of the Ninetyeast Ridge. Acta Geochimica, 2018, 37, 395-401.	1.7	18
50	Rare earth element abundances in presolar SiC. Geochimica Et Cosmochimica Acta, 2018, 221, 200-218.	3.9	9
51	The elemental abundances (with uncertainties) of the most Earth-like planet. Icarus, 2018, 299, 460-474.	2.5	63
52	Palaeoarchaean materials in the Tibetan Plateau indicated by zircon. International Geology Review, 2018, 60, 1061-1072.	2.1	8
53	Carbonated mantle domains at the base of the Earth's transition zone. Chemical Geology, 2018, 478, 69-75.	3.3	20
54	Experimental constraints on hydrogen diffusion in garnet. Contributions To Mineralogy and Petrology, 2018, 173, 1.	3.1	24

#	Article	IF	CITATIONS
55	Globally asynchronous sulphur isotope signals require re-definition of the Great Oxidation Event. Nature Communications, 2018, 9, 2245.	12.8	82
56	Halogens (F, Cl, Br, I) in Thirteen USCS, GSJ and NIST International Rock and Glass Reference Materials. Geostandards and Geoanalytical Research, 2018, 42, 499-511.	3.1	19
57	Adakitic rocks associated with the Shilu copper–molybdenum deposit in the Yangchun Basin, South China, and their tectonic implications. Acta Geochimica, 2017, 36, 132-150.	1.7	55
58	The limitations of hibonite as a single-mineral oxybarometer for early solar system processes. Chemical Geology, 2017, 466, 32-40.	3.3	11
59	Tracking the evolution of Late Mesozoic arc-related magmatic systems in Hong Kong using in-situ U-Pb dating and trace element analyses in zircon. American Mineralogist, 2017, 102, 2190-2219.	1.9	4
60	Zircon in amphibolites from Naxos, Aegean Sea, Greece: origin, significance and tectonic setting. Journal of Metamorphic Geology, 2017, 35, 413-434.	3.4	30
61	Inverted Oligoâ€Miocene metamorphism in the Lesser Himalaya Sequence, Arunachal Pradesh, India; age and grade relationships. Journal of Metamorphic Geology, 2016, 34, 805-820.	3.4	14
62	Zircon geochemistry of two contrasting types of eclogite: Implications for the tectonic evolution of the North Qaidam UHPM belt, northern Tibet. Gondwana Research, 2016, 35, 27-39.	6.0	49
63	Fluorine partitioning between eclogitic garnet, clinopyroxene, and melt at upper mantle conditions. Chemical Geology, 2016, 437, 88-97.	3.3	18
64	Generation of Late Mesozoic Qianlishan A 2 -type granite in Nanling Range, South China: Implications for Shizhuyuan W–Sn mineralization and tectonic evolution. Lithos, 2016, 266-267, 435-452.	1.4	130
65	Trace Element Content of Pyrite from the Kapai Slate, St. Ives Gold District, Western Australia. Economic Geology, 2016, 111, 1297-1320.	3.8	86
66	Oceanic anoxic events, subduction style and molybdenum mineralization. Solid Earth Sciences, 2016, 1, 64-73.	1.7	39
67	Rapid cooling of planetesimal core-mantle reaction zones from Mn-Cr isotopes in pallasites. Geochemical Perspectives Letters, 2016, , 68-77.	5.0	10
68	The Earth, Planets and Space Special Issue: "Science of solar system materials examined from Hayabusa and future missions― Earth, Planets and Space, 2015, 67, .	2.5	5
69	Synsedimentary to Early Diagenetic Gold in Black Shale-Hosted Pyrite Nodules at the Golden Mile Deposit, Kalgoorlie, Western Australia. Economic Geology, 2015, 110, 1157-1191.	3.8	70
70	Zircon U–Pb, O, and Hf isotopic constraints on Mesozoic magmatism in the Cyclades, Aegean Sea, Greece. International Journal of Earth Sciences, 2015, 104, 75-87.	1.8	44
71	The chemical conditions of the late Archean Hamersley basin inferred from whole rock and pyrite geochemistry with l"33S and l̃34S isotope analyses. Geochimica Et Cosmochimica Acta, 2015, 149, 223-250.	3.9	53
72	Mn–Cr dating of Fe- and Ca-rich olivine from â€~quenched' and â€~plutonic' angrite meteorites using Secondary Ion Mass Spectrometry. Geochimica Et Cosmochimica Acta, 2015, 157, 13-27.	3.9	19

5

#	Article	IF	CITATIONS
73	Secondary Ion Mass Spectrometry (SIMS). Encyclopedia of Earth Sciences Series, 2015, , 739-740.	0.1	1
74	Multiple Sulfur Isotope Analyses Support a Magmatic Model for the Volcanogenic Massive Sulfide Deposits of the Teutonic Bore Volcanic Complex, Yilgarn Craton, Western Australia. Economic Geology, 2015, 110, 1411-1423.	3.8	32
75	Sensitive high resolution ion microprobe – stable isotope (SHRIMP-SI) analysis of water in silicate glasses and nominally anhydrous reference minerals. Journal of Analytical Atomic Spectrometry, 2015, 30, 1706-1722.	3.0	17
76	The detrital zircon U–Pb–Hf fingerprint of the northern Arabian–Nubian Shield as reflected by a Late Ediacaran arkosic wedge (Zenifim Formation; subsurface Israel). Precambrian Research, 2015, 266, 1-11.	2.7	51
77	Preservation of a fragmented late Neoproterozoic–earliest Cambrian hyper-extended continental-margin sequence in the Australian Delamerian Orogen. Geological Society Special Publication, 2015, 413, 269-299.	1.3	12
78	The Pounamu terrane, a new Cretaceous exotic terrane within the Alpine Schist, New Zealand; tectonically emplaced, deformed and metamorphosed during collision of the LIP Hikurangi Plateau with Zealandia. Gondwana Research, 2015, 27, 1255-1269.	6.0	21
79	Gondwana margin evolution from zircon REE, O and Hf signatures of Western Province gneisses, Zealandia. Geological Society Special Publication, 2015, 389, 323-353.	1.3	12
80	Timing of global crustal metamorphism on Vesta as revealed by high-precision U–Pb dating and trace element chemistry of eucrite zircon. Earth and Planetary Science Letters, 2015, 409, 182-192.	4.4	39
81	Stellar Chronology. Encyclopedia of Earth Sciences Series, 2015, , 780-781.	0.1	0
82	Secondary Ion Mass Spectrometry. New Developments in Mass Spectrometry, 2014, , 439-499.	0.2	9
83	U–Pb geochronology of Permian plutonic rocks, Longwood Range, New Zealand: implications for Median Batholith–Brook Street Terrane relations. New Zealand Journal of Geology, and Geophysics, 2014, 57, 65-85.	1.8	36
84	The genetic association between magnetite–hematite and porphyry copper deposits: Reply to Pokrovski. Geochimica Et Cosmochimica Acta, 2014, 126, 639-642.	3.9	9
85	Paragenesis and composition of ore minerals in the Randalls BIF-hosted gold deposits, Yilgarn Craton, Western Australia: Implications for the timing of deposit formation and constraints on gold sources. Precambrian Research, 2014, 243, 110-132.	2.7	23
86	Stratigraphy and structure of the Ngatamariki geothermal system from new zircon U–Pb geochronology: Implications for Taupo Volcanic Zone evolution. Journal of Volcanology and Geothermal Research, 2014, 274, 51-70.	2.1	61
87	Charge-mode electrometer measurements of S-isotopic compositions on SHRIMP-SI. International Journal of Mass Spectrometry, 2014, 359, 26-37.	1.5	60
88	New Perspectives on the Bishop Tuff from Zircon Textures, Ages and Trace Elements. Journal of Petrology, 2014, 55, 395-426.	2.8	96
89	Post-supereruption Magmatic Reconstruction of Taupo Volcano (New Zealand), as Reflected in Zircon Ages and Trace Elements. Journal of Petrology, 2014, 55, 1511-1533.	2.8	49
90	Temporal evolution and compositional signatures of two supervolcanic systems recorded in zircons from Mangakino volcanic centre, New Zealand. Contributions To Mineralogy and Petrology, 2014, 167, 1.	3.1	32

#	Article	IF	CITATIONS
91	Magnetite–hematite, oxygen fugacity, adakite and porphyry copper deposits: Reply to Richards. Geochimica Et Cosmochimica Acta, 2014, 126, 646-649.	3.9	14
92	Provenance connections between late Neoproterozoic and early Palaeozoic sedimentary basins of the Ross Sea region, Antarctica, south-east Australia and southern Zealandia. Antarctic Science, 2014, 26, 173-182.	0.9	28
93	Ba isotopic compositions in stardust SiC grains from the Murchison meteorite: Insights into the stellar origins of large SiC grains. Geochimica Et Cosmochimica Acta, 2013, 120, 628-647.	3.9	15
94	Mn–Cr relative sensitivity Factors for Secondary Ion Mass Spectrometry analysis of Mg–Fe–Ca olivine and implications for the Mn–Cr chronology of meteorites. Geochimica Et Cosmochimica Acta, 2013, 110, 216-228.	3.9	12
95	A re-evaluation of the Mn–Cr systematics of olivine from the angrite meteorite D'Orbigny using Secondary Ion Mass Spectrometry. Geochimica Et Cosmochimica Acta, 2013, 123, 181-194.	3.9	7
96	The link between reduced porphyry copper deposits and oxidized magmas. Geochimica Et Cosmochimica Acta, 2013, 103, 263-275.	3.9	339
97	U–Pb dating of zircon in hydrothermally altered rocks of the Kawerau Geothermal Field, Taupo Volcanic Zone, New Zealand. Journal of Volcanology and Geothermal Research, 2013, 253, 97-113.	2.1	30
98	Dating the Oldest Rocks and Minerals in the Solar System. Elements, 2013, 9, 39-44.	0.5	30
99	Invited Review Article: Recent developments in isotope-ratio mass spectrometry for geochemistry and cosmochemistry. Review of Scientific Instruments, 2013, 84, 011101.	1.3	37
100	EUROPIUM <i>s</i> -PROCESS SIGNATURE AT CLOSE-TO-SOLAR METALLICITY IN STARDUST SIC GRAINS FROM ASYMPTOTIC GIANT BRANCH STARS. Astrophysical Journal Letters, 2013, 768, L18.	8.3	14
101	No mass-independent sulfur isotope fractionation in auriferous fluids supports a magmatic origin for Archean gold deposits. Geology, 2013, 41, 791-794.	4.4	92
102	Magnetocentrifugal jets and chondrule formation in protostellar disks. Proceedings of the International Astronomical Union, 2013, 8, 228-229.	0.0	0
103	Oxygen isotope tracing of the Solar System. Australian Journal of Earth Sciences, 2012, 59, 225-236.	1.0	9
104	Is the switch from I- to S-type magmatism in the Himalayan Orogen indicative of the collision of India and Eurasia?. Australian Journal of Earth Sciences, 2012, 59, 321-340.	1.0	19
105	TUNGSTEN ISOTOPIC COMPOSITIONS IN STARDUST SIC GRAINS FROM THE MURCHISON METEORITE: CONSTRAINTS ON THE <i>s</i> -PROCESS IN THE Hf-Ta-W-Re-Os REGION. Astrophysical Journal, 2012, 744, 49.	4.5	32
106	Mylonites of the South Armorican Shear Zone: Insights for crustal-scale fluid flow and water–rock interaction processes. Journal of Geodynamics, 2012, 56-57, 86-107.	1.6	43
107	Formation of chondrules in magnetic winds blowing through the proto-asteroid belt. Earth and Planetary Science Letters, 2012, 327-328, 61-67.	4.4	29
108	High-uranium matrix effect in zircon and its implications for SHRIMP U–Pb age determinations. Chemical Geology, 2012, 306-307, 78-91.	3.3	189

#	Article	IF	CITATIONS
109	The role of protostellar jets in star formation and the evolution of the early solar system: Astrophysical and meteoritical perspectives. Meteoritics and Planetary Science, 2012, 47, 1922-1940.	1.6	6
110	CAN GALACTIC CHEMICAL EVOLUTION EXPLAIN THE OXYGEN ISOTOPIC VARIATIONS IN THE SOLAR SYSTEM?. Astrophysical Journal, 2012, 759, 51.	4.5	7
111	Where does India end and Eurasia begin?. Geochemistry, Geophysics, Geosystems, 2011, 12, n/a-n/a.	2.5	3
112	Deconvolving episodic age spectra from zircons of the Ladakh Batholith, northwest Indian Himalaya. Chemical Geology, 2011, 289, 179-196.	3.3	64
113	Simultaneous resetting of the muscovite Kâ€Ar and monazite Uâ€Pb geochronometers: a story of fluids. Terra Nova, 2011, 23, 390-398.	2.1	45
114	Petrology and geochemistry of dunites, chromitites and mineral inclusions from the Gaositai Alaskan-type complex, North China Craton: Implications for mantle source characteristics. Lithos, 2011, 127, 165-175.	1.4	30
115	Arc–continent collision and orogenesis in western Tasmanides: Insights from reactivated basement structures and formation of an ocean–continent transform boundary off western Tasmania. Gondwana Research, 2011, 19, 608-627.	6.0	64
116	Autochthonous inheritance of zircon through Cretaceous partial melting of Carboniferous plutons: the Arthur River Complex, Fiordland, New Zealand. Contributions To Mineralogy and Petrology, 2011, 161, 401-421.	3.1	20
117	Oxygen Isotopic Compositions of Asteroidal Materials Returned from Itokawa by the Hayabusa Mission. Science, 2011, 333, 1116-1119.	12.6	161
118	Three-Dimensional Structure of Hayabusa Samples: Origin and Evolution of Itokawa Regolith. Science, 2011, 333, 1125-1128.	12.6	249
119	Irradiation History of Itokawa Regolith Material Deduced from Noble Gases in the Hayabusa Samples. Science, 2011, 333, 1128-1131.	12.6	128
120	Neutron Activation Analysis of a Particle Returned from Asteroid Itokawa. Science, 2011, 333, 1119-1121.	12.6	55
121	Field and Geochemical Constraints on Mafic-Felsic Interactions, and Processes in High-level Arc Magma Chambers: an Example from the Halfmoon Pluton, New Zealand. Journal of Petrology, 2010, 51, 1477-1505.	2.8	68
122	U–Pb chronology of the Solar System's oldest solids with variable 238U/235U. Earth and Planetary Science Letters, 2010, 300, 343-350.	4.4	270
123	U-Th-Pb zircon and monazite geochronology of Western Province gneissic rocks, central-south Westland, New Zealand. New Zealand Journal of Geology, and Geophysics, 2010, 53, 241-269.	1.8	18
124	Microinclusions in monocrystalline octahedral diamonds and coated diamonds from Diavik, Slave Craton: Clues to diamond genesis. Lithos, 2009, 112, 724-735.	1.4	31
125	Geochemistry and Os–Nd–Sr isotopes of the Gaositai Alaskan-type ultramafic complex from the northern North China craton: implications for mantle–crust interaction. Contributions To Mineralogy and Petrology, 2009, 158, 683-702.	3.1	65
126	Mass-spectrometric mining of Hadean zircons by automated SHRIMP multi-collector and single-collector U/Pb zircon age dating: The first 100,000 grains. International Journal of Mass Spectrometry, 2009, 286, 53-63.	1.5	158

#	Article	IF	CITATIONS
127	Origin of Lower Cretaceous (â€~Nubian') sandstones of Northâ€east Africa and Arabia from detrital zircon Uâ€Pb SHRIMP dating. Sedimentology, 2009, 56, 2010-2023.	3.1	29
128	lsotopic records in CM hibonites: Implications for timescales of mixing of isotope reservoirs in the solar nebula. Geochimica Et Cosmochimica Acta, 2009, 73, 5051-5079.	3.9	113
129	IRASÂ22036+5306: an Al ₂ O ₃ oxide-dominated post-AGB star. Monthly Notices of the Royal Astronomical Society, 2008, 386, 2290-2296.	4.4	9
130	Determining high precision, in situ, oxygen isotope ratios with a SHRIMP II: Analyses of MPI-DING silicate-glass reference materials and zircon from contrasting granites. Chemical Geology, 2008, 257, 114-128.	3.3	254
131	Development of SHRIMP. Australian Journal of Earth Sciences, 2008, 55, 937-954.	1.0	76
132	Oxygen in the Sun. Reviews in Mineralogy and Geochemistry, 2008, 68, 73-92.	4.8	10
133	6. Oxygen in the Sun. , 2008, , 73-92.		3
134	Allanite micro-geochronology: A LA-ICP-MS and SHRIMP U–Th–Pb study. Chemical Geology, 2007, 245, 162-182.	3.3	122
135	Loch Burn Formation, Fiordland, New Zealand: SHRIMP Uâ€Pb ages, geochemistry and provenance. New Zealand Journal of Geology, and Geophysics, 2007, 50, 167-180.	1.8	18
136	SHRIMP ion probe zircon geochronology and Sr and Nd isotope geochemistry for southern Longwood Range and Bluff Peninsula intrusive rocks of Southland, New Zealand. New Zealand Journal of Geology, and Geophysics, 2006, 49, 291-303.	1.8	25
137	Isotopic enhancements of 170 and 180 from solar wind particles in the lunar regolith. Nature, 2006, 440, 776-778.	27.8	71
138	Provenance of Cambrian conglomerates from New Zealand: implications for the tectonomagmatic evolution of the SE Gondwana margin. Journal of the Geological Society, 2006, 163, 997-1010.	2.1	17
139	Al2O3 dust in OH/IR stars. Monthly Notices of the Royal Astronomical Society, 2005, 362, 872-878.	4.4	14
140	The Paleozoicâ€Mesozoic recycling of the Rakaia Terrane, South Island, New Zealand: Sandstone clast and sandstone petrology, geochemistry, and geochronology. New Zealand Journal of Geology, and Geophysics, 2005, 48, 229-245.	1.8	13
141	SIMS Measurement of Stable Isotopes. , 2004, , 652-691.		12
142	The regional significance of Cretaceous magmatism and metamorphism in Fiordland, New Zealand, from U-Pb zircon geochronology. Journal of Metamorphic Geology, 2004, 22, 607-627.	3.4	59
143	Provenance analysis using conglomerate clast lithologies: a case study from the Pahau terrane of New Zealand. Sedimentary Geology, 2004, 167, 57-89.	2.1	62
144	Provenance of the sedimentary Rakaia sub-terrane, Torlesse Terrane, South Island, New Zealand: the use of igneous clast compositions to define the source. Sedimentary Geology, 2004, 168, 193-226.	2.1	36

#	Article	lF	CITATIONS
145	Provenance of the sedimentary Rakaia sub-terrane, Torlesse Terrane, South Island, New Zealand: the use of igneous clast compositions to define the source. Sedimentary Geology, 2004, 168, 193-193.	2.1	3
146	Geochronology and geochemistry of highâ€pressure granulites of the Arthur River Complex, Fiordland, New Zealand: Cretaceous magmatism and metamorphism on the palaeoâ€Pacific Margin. Journal of Metamorphic Geology, 2003, 21, 299-313.	3.4	60
147	Considerations in Zircon Geochronology by SIMS. Reviews in Mineralogy and Geochemistry, 2003, 53, 215-241.	4.8	318
148	Initial 182Hf/180Hf in meteoritic zircons. Geochimica Et Cosmochimica Acta, 2003, 67, 4849-4856.	3.9	16
149	Evaluation of Duluth Complex anorthositic series (AS3) zircon as a U-Pb geochronological standard: new high-precision isotope dilution thermal ionization mass spectrometry results. Geochimica Et Cosmochimica Acta, 2003, 67, 3665-3672.	3.9	130
150	Tectonics of the Qinling (Central China): tectonostratigraphy, geochronology, and deformation history. Tectonophysics, 2003, 366, 1-53.	2.2	768
151	8. Considerations in Zircon Geochronology by SIMS. , 2003, , 215-242.		51
152	Timing of deposition, orogenesis and glaciation within the Dalradian rocks of Scotland: constraints from U–Pb zircon ages. Journal of the Geological Society, 2002, 159, 83-94.	2.1	145
153	Constraints on the age of formation of seismically reflective middle and lower crust beneath the Bering Shelf: SHRIMP zircon dating of xenoliths from Saint Lawrence Island. , 2002, , .		4
154	Low δ18O zircons, U-Pb dating, and the age of the Qinglongshan oxygen and hydrogen isotope anomaly near Donghai in Jiangsu Province, China. Geochimica Et Cosmochimica Acta, 2002, 66, 2299-2306.	3.9	154
155	Geological and chronological evidence of Indo-Chinese strike- slip movement in the Altyn Tagh fault zone. Science Bulletin, 2002, 47, 27.	1.7	18
156	Relationship between Granite and Eclogite on the Southern Margin of the Qilian Mountains: Evidence from Zircon SHRIMP Ages of the Aolaoshan Granite. Acta Geologica Sinica, 2002, 76, 118-125.	1.4	5
157	Late Pleistocene granodiorite beneath Crater Lake caldera, Oregon, dated by ion microprobe. Geology, 2000, 28, 467.	4.4	63
158	Zircon U–Pb sensitive high massâ€resolution ion microprobe dating of granitoids in the Ryoke metamorphic belt, Kinki District, Southwest Japan. Island Arc, 2000, 9, 55-63.	1.1	18
159	Exhumation of ultrahigh-pressure continental crust in east central China: Late Triassic-Early Jurassic tectonic unroofing. Journal of Geophysical Research, 2000, 105, 13339-13364.	3.3	608
160	Exhumation of the ultrahigh-pressure continental crust in east central China: Cretaceous and Cenozoic unroofing and the Tan-Lu fault. Journal of Geophysical Research, 2000, 105, 13303-13338.	3.3	346
161	Rare earth element chemistry of zircon and its use as a provenance indicator. Geology, 2000, 28, 627.	4.4	738
162	The Solar System's Earliest Chemistry: Systematics of Refractory Inclusions. International Geology Review, 2000, 42, 865-894.	2.1	62

#	Article	IF	CITATIONS
163	Rare earth element chemistry of zircon and its use as a provenance indicator. Geology, 2000, 28, 627-630.	4.4	54
164	Late Pleistocene granodiorite beneath Crater Lake caldera, Oregon, dated by ion microprobe. Geology, 2000, 28, 467-470.	4.4	2
165	New insight into the dynamic development of the Southern Alps, New Zealand, from detailed thermochronological investigation of the Mataketake Range pegmatites. Geological Society Special Publication, 1999, 154, 261-282.	1.3	17
166	ISOTOPE GEOCHEMISTRY:New Tools for Isotopic Analysis. Science, 1999, 286, 2289-2290.	12.6	7
167	Black Giants Anorthosite, New Zealand: A Paleozoic analogue of Archean stratiform anorthosites and implications for the formation of Archean high-grade gneiss terranes. Geology, 1999, 27, 131.	4.4	27
168	SHRIMP monazite and zircon geochronology of highâ€grade metamorphism in New Zealand. Journal of Metamorphic Geology, 1998, 16, 149-167.	3.4	138
169	Regional implications of U/Pb SHRIMP age constraints on the tectonic evolution of New Caledonia. Tectonophysics, 1998, 299, 333-343.	2.2	63
170	U/Pb zircon ages constrain the architecture of the ultrahigh-pressure Qinling–Dabie Orogen, China. Earth and Planetary Science Letters, 1998, 161, 215-230.	4.4	877
171	U-Pb, Th-Pb and Ar-Ar geochronology from the southern Sierras Pampeanas, Argentina: implications for the Palaeozoic tectonic evolution of the western Gondwana margin. Geological Society Special Publication, 1998, 142, 259-281.	1.3	110
172	Geochronology and geochemistry of a Mesozoic magmatic arc system, Fiordland, New Zealand. Journal of the Geological Society, 1998, 155, 1037-1053.	2.1	159
173	Development of the early Paleozoic Pacific margin of Gondwana from detrital-zircon ages across the Delamerian orogen. Geology, 1998, 26, 243.	4.4	275
174	Basement geology of Taranaki and Wanganui Basins, New Zealand. New Zealand Journal of Geology, and Geophysics, 1997, 40, 223-236.	1.8	97
175	A Caledonian age for the Kiloran Bay appinite intrusion on Colonsay, Inner Hebrides. Scottish Journal of Geology, 1997, 33, 75-83.	0.1	8
176	Detrital zircon age patterns and provenance in late Paleozoic–early Mesozoic New Zealand terranes and development of the paleo-Pacific Gondwana margin. Geology, 1997, 25, 939.	4.4	55
177	Field characteristics, petrography, and geochronology of the Hohonu Batholith and the adjacent Granite Hill Complex, North Westland, New Zealand. New Zealand Journal of Geology, and Geophysics, 1997, 40, 1-17.	1.8	59
178	SHRIMP Uâ€Pb geochronology of Cretaceous magmatism in northwest Nelsonâ€Westland, South Island, New Zealand. New Zealand Journal of Geology, and Geophysics, 1997, 40, 453-463.	1.8	73
179	Equilibration and reaction in Archaean quartz-sapphirine granulite xenoliths from the Lace kimberlite pipe, South Africa. Journal of Metamorphic Geology, 1997, 15, 253-266.	3.4	35
180	Ion microprobe dating of Paleozoic granitoids: Devonian magmatism in New Zealand and correlations with Australia and Antarctica. Chemical Geology, 1996, 127, 191-210.	3.3	118

#	Article	IF	CITATIONS
181	The Search for Interstellar Components in Interplanetary Dust Particles. International Astronomical Union Colloquium, 1996, 150, 275-282.	0.1	10
182	Extension of Delamerian (Ross) orogen into western New Zealand: Evidence from zircon ages and implications for crustal growth along the Pacific margin of Gondwana. Geology, 1996, 24, 1087.	4.4	94
183	Geochemistry of the Karamea Batholith, New Zealand and comparisons with the Lachlan Fold Belt granites of SE Australia. Lithos, 1996, 39, 1-20.	1.4	66
184	Ages of Silurian radiolarians from the Kurosegawa terrane, southwest Japan constrained by U/Pb SHRIMP data. Journal of Southeast Asian Earth Sciences, 1996, 14, 53-70.	0.2	39
185	A tale of two eras: Pliocene-Pleistocene unroofing of Cenozoic and late Archean zircons from active metamorphic core complexes, Solomon Sea, Papua New Guinea. Geology, 1995, 23, 1023.	4.4	61
186	Granulite formation during continental extension in Fiordland, New Zealand. Nature, 1995, 375, 479-482.	27.8	83
187	Age profile of ophiolitic rocks across the Late Palaeozoic New England Orogen, New South Wales: Implications for tectonic models. Australian Journal of Earth Sciences, 1995, 42, 11-23.	1.0	72
188	Trace elements in diamond inclusions from eclogites reveal link to Archean granites. Earth and Planetary Science Letters, 1994, 128, 199-213.	4.4	145
189	lon microprobe Uî—,Pb zircon geochronology of granitic magmatism in the Western Province of the South Island, New Zealand. Chemical Geology, 1994, 113, 171-189.	3.3	87
190	Carbon, nitrogen, magnesium, silicon, and titanium isotopic compositions of single interstellar silicon carbide grains from the Murchison carbonaceous chondrite. Astrophysical Journal, 1994, 430, 870.	4.5	214
191	Isotopically normal zirconium in Murchison hibonite 13-13: Implications for a link between the e- and r-processes. Astrophysical Journal, 1994, 434, L79.	4.5	3
192	Intraplate origin of komatiites inferred from trace elements in glass inclusions. Nature, 1993, 365, 432-434.	27.8	91
193	530 Ma zircon age for ophiolite from the New England orogen: Oldest rocks known from eastern Australia. Geology, 1992, 20, 125.	4.4	57
194	Crustal evolution of New Zealand: Evidence from age distributions of detrital zircons in Western Province paragneisses and Torlesse greywacke. Geochimica Et Cosmochimica Acta, 1992, 56, 911-920.	3.9	120
195	Evidence for distillation in the formation of HAL and related hibonite inclusions. Geochimica Et Cosmochimica Acta, 1992, 56, 2503-2520.	3.9	87
196	The oldest zircons in the solar system. Earth and Planetary Science Letters, 1992, 109, 1-10.	4.4	141
197	Hibonite-bearing microspherules: A new type of refractory inclusions with large isotopic anomalies. Geochimica Et Cosmochimica Acta, 1991, 55, 367-379.	3.9	86
198	Isotopically anomalous TI in presolar SiC from the Murchison meteorite. Astrophysical Journal, 1991, 376, L53.	4.5	43

#	Article	IF	CITATIONS
199	Presolar isotopic and chemical signatures in hibonite-bearing refractory inclusions from the Murchison carbonaceous chondrite. Geochimica Et Cosmochimica Acta, 1990, 54, 3219-3237.	3.9	135
200	U-Th-Pb systematics of individual perovskite grains from the Allende and Murchison carbonaceous chondrites. Earth and Planetary Science Letters, 1990, 101, 379-387.	4.4	43
201	Chromium isotopic anomalies in the Murchison meteorite. Earth and Planetary Science Letters, 1989, 92, 1-6.	4.4	19
202	Comment and Reply on "Age constraints on metamorphism and the development of a metamorphic core complex in Fiordland, southern New Zealand". Geology, 1989, 17, 380.	4.4	19
203	Correlated morphological, chemical, and isotopic characteristics of hibonites from the Murchison carbonaceous chondrite. Geochimica Et Cosmochimica Acta, 1988, 52, 2827-2839.	3.9	129
204	Trace-element abundances in hibonites from the Murchison carbonaceous chondrite: Constraints on high-temperature processes in the solar nebula. Geochimica Et Cosmochimica Acta, 1988, 52, 2841-2854.	3.9	76
205	Early archaean zircon ages from orthogneisses and anorthosites at Mount Narryer, Western Australia. Precambrian Research, 1988, 38, 325-341.	2.7	131
206	Age constraints on metamorphism and the development of a metamorphic core complex in Fiordland, southern New Zealand. Geology, 1988, 16, 405.	4.4	121
207	Large heterogeneous 26Mg excesses in a hibonite from the Murchison meteorite. Nature, 1987, 327, 689-692.	27.8	25
208	Magnesium isotopic compositions of olivine, spinel, and hibonite from the Murchison carbonaceous chondrite. Geochimica Et Cosmochimica Acta, 1986, 50, 1413-1421.	3.9	24
209	Large Ca-48 anomalies are associated with Ti-50 anomalies in Murchison and Murray hibonites. Astrophysical Journal, 1986, 311, L103.	4.5	74
210	The age of (a tiny part of) the Australian continent. Nature, 1985, 317, 559-560.	27.8	28
211	Titanium isotopic anomalies in hibonites from the Murchison carbonaceous chondrite. Geochimica Et Cosmochimica Acta, 1985, 49, 1989-1993.	3.9	37
212	Unsupported radiogenic Pb in zircon: a cause of anomalously high Pb-Pb, U-Pb and Th-Pb ages. Contributions To Mineralogy and Petrology, 1984, 88, 322-327.	3.1	243
213	Ion microprobe identification of 4,100–4,200 Myr-old terrestrial zircons. Nature, 1983, 304, 616-618.	27.8	460